

DOI: 10.1002/sml.200700033

Semiconducting Cyanide–Transition-Metal Nanotubes

Yina Mo and Efthimios Kaxiras*

We propose a new type of structurally simple and energetically stable cyanide–transition-metal nanotube, based on the planar structure of $M(\text{CN})_2$ ($M = \text{Ni}, \text{Pd}, \text{Pt}$). These nanotubes have a semiconducting character with a large bandgap (2–3 eV) that is insensitive to chirality and diameter. The energetic, electronic, and mechanical properties of these materials in both planar and tubular forms are studied through first-principles density functional theory calculations. The calculations reveal interesting multicenter bonding features, which should lead to preferential growth of tubes of a particular chirality. These intrinsically semiconducting nanotubes can be readily *p*- or *n*-doped, which makes them good candidates for nanoscale elements in electronic devices.

Keywords:

- ab initio calculations
- electronic structure
- nanotubes
- semiconductors
- transition metals

1. Introduction

The discovery of carbon nanotubes (CNTs)^[1] has given birth to an entire field devoted to the study of these one-dimensional (1D) nanoscale structures that exhibit extraordinary properties and promise for applications. For instance, single-walled CNTs have been reported to show Luttinger liquid behavior^[2] and proximity in proximity-induced superconductivity.^[3] The electronic properties of a CNT are fully determined by its chirality and can range from metallic to semiconducting. Control of the nanotube chirality and diameter during growth is difficult and presents a major obstacle to mass production of nanotubes with desired properties. To overcome this limitation, boron nitride nanotubes (BNTs), which have properties less sensitive to chirality, were proposed theoretically^[4] and later realized experimentally.^[5]

Herein, we propose a new type of structurally simple and energetically stable nanotube consisting of transition-metal atoms and cyanide units. To examine the structural and electronic properties of the cyanide compounds and nanotubes, we employ density functional theory (DFT) as implemented in VASP,^[6–8] with computational parameters that ensure high accuracy.^[9] We find that the cyanide–transi-

tion-metal nanotubes are semiconductors with large bandgaps (2–3 eV), and that their chirality affects the electronic bandgap only marginally. The nature of bonding in these systems suggests that tubes of a particular chirality will be energetically more stable, thus leading to a natural self-selection of tubes with well-defined electronic properties.

The cyanide compounds we consider are composed of the transition metals Ni, Pd, or Pt in their 2+ oxidation state and the cyanide base $(\text{CN})^-$. The simplest possible structure consisting of these structural units, suggested by Pauling,^[10] is shown in Figure 1a; we refer to this as structure I. The unit cell contains one metal atom and two CN units. Each metal atom is surrounded by two C and two N atoms, with the two C atoms being second neighbors (similarly for the two N atoms). There are two other ways of arranging the atoms in the ab initio calculation square-planar lattice, but with larger unit cells. In the first, shown in Figure 1b and called structure IIa, there are two metal atoms and four CN units in each unit cell, with one metal atom surrounded by four C atoms and the other by four N atoms. In the second, shown in Figure 1c and called structure IIb, which also contains two metal atoms and four CN units in the unit cell, each metal atom is surrounded by two C and two N atoms and the pattern is rotated by 90° in neighboring metal sites. The two C neighbors of a given metal atom are not second but third nearest neighbors (similarly for the two N atoms); the second neighbors are the C and N atoms belonging to different CN units. In all structures, the metal and CN units are linked by strong covalent bonds, while the

[*] Y. Mo, Prof. E. Kaxiras
Physics Department and School of Engineering and Applied Sciences, Lyman Laboratory
Harvard University
17 Oxford Street, Cambridge, MA 02138 (USA)
Fax: (+1) 617-496-2545
E-mail: kaxiras@physics.harvard.edu

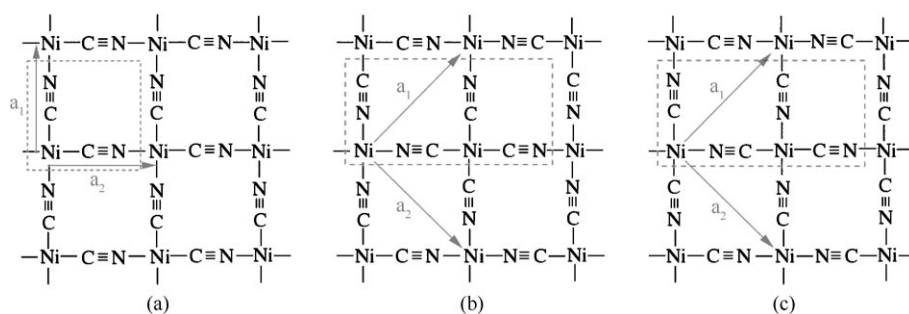


Figure 1. The three types of $\text{Ni}(\text{CN})_2$ sheet (the Ni atoms can be replaced by Pd or Pt atoms for $\text{Pd}(\text{CN})_2$ or $\text{Pt}(\text{CN})_2$ sheets) with the corresponding primitive lattice vectors \mathbf{a}_1 , \mathbf{a}_2 , and atomic basis (enclosed within the dashed lines).

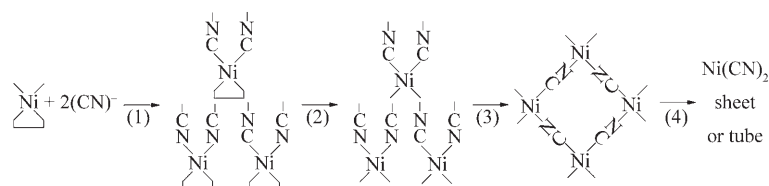
interplanar interactions are weaker and of the van der Waals type. Of these, the type IIa $\text{Ni}(\text{CN})_2$ planar structure was experimentally reported more than a century ago,^[11] formed in ammonia solution; its structure has been studied in detail.^[12]

2. Results and Discussion

2.1. Structural Features

Our DFT calculations indicate that structure I, although to our knowledge not yet reported experimentally, is the lowest-energy structure. In the case of Ni, structure IIa has a higher energy than structure I by 0.07 eV per $\text{Ni}(\text{CN})_2$ unit; structure IIb has a higher energy than structure I by 0.17 eV per $\text{Ni}(\text{CN})_2$ unit. Thus, structure I is the thermodynamically stable one, although its formation under hydrothermal conditions in ammonia solution may have been kinetically inhibited. By using modern synthetic methods, it should be possible to form structure I by gas-phase reactions. A potential reaction sequence is indicated in Scheme 1.

The synthesis starts by using chelating agents to clamp two of the possible bonds of each Ni atom that is in its square-planar coordination, which leaves the remaining two free to react. The product of this initial step in the reaction process is shown schematically as the initial configuration in Scheme 1. Next, the cyanide bases $(\text{CN})^-$ are added. These bases react in the gas phase with the clamped Ni atoms and three possible products, shown in Scheme 1 after step 1. The chelating agent is removed (step 2) and the $\text{Ni}(\text{CN})_2$ molecules are free to react with each other (step 3) to form



Scheme 1. Gas-phase synthesis of $\text{Ni}(\text{CN})_2$ sheet and nanotubes. See text for details of the four steps in the process.

larger units, eventually growing to become the extended planar structure (step 4). During this last step in the reaction, the lowest-energy structure I (Figure 1a) should be naturally chosen, although structures IIa and IIb or even structures with less order could be formed from a mixture of the three structural units produced by step 2 of the reaction path. Our calculations show that the electronic properties of the three planar structures are very

similar, which indicates that disorder will not affect the electronic behavior significantly. If a planar structure can be formed, the same synthetic procedure could lead to the formation of nanotubes, as is the case for the CNTs and BNTs. Accordingly, in the following we concentrate on the properties of planar and tubular structures based on structure I.

The square-lattice structure of the cyanide sheet has lower symmetry than the hexagonal structure of a single graphite sheet (graphene), which effectively reduces the possible ways of rolling it into tubes. We will concentrate on the three simplest types of tube (see Figure 2): the $(n,0)$ tubes, which correspond to rolling the sheet along one of the lattice vector directions, and the (n,n) or (n,\bar{n}) tubes, which correspond to rolling the sheet along the two diagonal directions of the unit cell. Notice that the two diagonal directions are not equivalent: the (n,n) tubes correspond to cross sections involving a metal atom bonded to one C and one N atom, whereas the (n,\bar{n}) tubes correspond to cross sections involving a metal atom bonded to two atoms of the same type (both C or both N, depending on where the cross section is taken). Two examples (the $(4,0)$ and $(4,\bar{4})$ nanotubes) are shown in Figure 2. A general chirality (n,m) is also allowed in principle, but the stability of such tubes may be inhibited by the complexity of bonding between the metal atoms and the cyanide units.

2.2. Electronic Features

We consider next the electronic properties of the cyanide sheets and nanotubes. It is found that the band structures of the sheets with different metal elements are very similar. When the sheets are rolled into 1D structures, the overall band-structure features remain similar to those of the corresponding sheet structure, aside from the folding of the 2D Brillouin zone (BZ) of the sheet to the 1D zone of the tube. Accordingly, we present here only a detailed analysis of the band-structure and bonding fea-

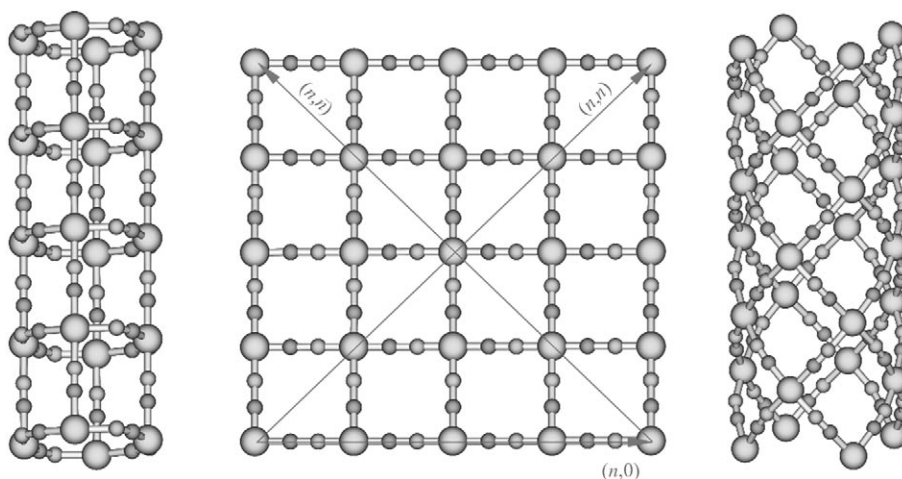


Figure 2. Top view of the sheet (center, a 4×4 area) and the $(4,0)$ (left) and $(4,\bar{4})$ (right) nanotubes based on structure I. Diagonal and horizontal arrows indicate the $(n,0)$, (n,n) , and (n,\bar{n}) tube-rolling directions. Large spheres: metal; small, light-gray spheres: N; small, dark-gray spheres: C

tures of the $\text{Ni}(\text{CN})_2$ sheet, which is representative of all other cyanide planar and tubular structures.

Figure 3 shows the band structure (left) and the magnitude of the wave function (right) of various bands at Γ , the BZ center. There are 14 filled bands; the lowest two correspond to C–N σ bonds and their energy lies below the range shown in Figure 3. The band structure shown contains the other 12 filled bands and three of the conduction bands. The bandgap (2 eV) is indirect, between Γ and the high-symmetry point M. Of the 15 bands shown, four are denoted by open circles (bands 7–10, unlabeled in Figure 3), which lie in the range between -2 and -4 eV; these states correspond to four C–N bonds of pure π character which, together with the C–N σ bonds, form the triple bond between these two atoms of the cyanide unit. The remaining 11 bands are denoted by filled circles and correspond to bonds involving both s and p orbitals of C and N, as well as

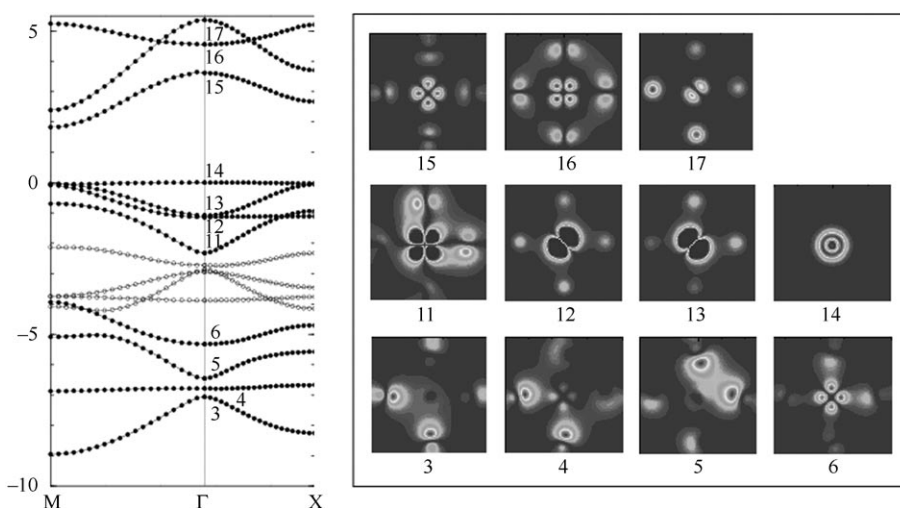


Figure 3. Left: band structure of the $\text{Ni}(\text{CN})_2$ sheet; the Fermi level is at the highest-occupied band. Right: plots of $|\Phi(r)|^2$ for the wave function at Γ that include significant contributions from Ni d orbitals (see text).

d orbitals from the metal atoms. We classify these bands into three categories:

- 1) Bands 3–6 lie in the energy range -4 to $+9$ eV and correspond to N–N (band 3) and C–C (band 5) interactions, and to N–Ni–N (band 4) and C–Ni–C (band 6) bonds. All of these interactions have σ character; the last two are three-center bonds.
- 2) Bands 11–13 lie in the energy range -2 to 0 eV, and correspond to multiple center bonds of π character: band 11 involves all five atoms in the unit cell (a five-center bond), band 12 involves the two N atoms and the Ni atom (a three-center bond), and band 13 involves the two C atoms and the Ni atom (another three-center bond). Band 14 corresponds to a non-bonding state of Ni of $d_{3z^2-r^2}$ character; this last band is the highest-occupied one and exhibits no dispersion, since it does not involve interaction with any of the other orbitals.
- 3) The remaining three bands are unoccupied, and correspond to the antibonding combinations of states that were already encountered in the valence manifold, as is evident from the wave-function features.

The band structure described above can be accurately reproduced by a tight-binding scheme with a minimal basis consisting of the four sp orbitals of C, the four sp orbitals of N, and the five d orbitals of Ni. A detailed interpretation of the character of the bands is provided in Table 1. The participation of d orbitals introduces two groups of interesting multicenter interactions:

the relatively weak five-center π interactions (bands 11–13) and the considerably stronger three-center σ interactions (bands 4 and 6). Interrupting or distorting these interactions would incur large energy costs. Based on this observation, we predict that the (n,n) and (n,\bar{n}) diagonal tubes will have lower energy than the $(n,0)$ square tubes, because rolling the sheet along the diagonal direction introduces smaller distortion

Table 1. Interpretation of electronic states at Γ , in terms of transition-metal d orbitals and C, N s and p orbitals (see text for details). σ and π stand for the character of the interactions; α to ζ are coefficients that determine the weight of each orbital in the electronic state (an overall normalization factor is omitted).

n	Ni orbitals C, N orbitals	Character
17	$(d_{yz} + d_{zx}) - [\gamma(p_z^{C_1} - p_z^{C_2}) - \delta(p_z^{N_1} - p_z^{N_2})]$	antibonding
16	$d_{xy} - [\alpha(p_y^{C_1} + p_x^{C_2}) - \beta(p_y^{N_1} + p_x^{N_2})]$	antibonding
15	$d_{x^2-y^2} - \xi[(s^{C_1} - p_x^{C_1}) - (s^{C_2} - p_y^{C_2})]$	antibonding
14	$d_{x^2-3z^2}$	nonbonding
13	$(d_{yz} - d_{zx}) + [\delta(p_z^{C_1} - p_z^{C_2}) + \gamma(p_z^{N_1} - p_z^{N_2})]$	$C_{1,2}$ -Ni- $N_{1,2}$ (π)
12	$(d_{yz} + d_{zx}) + [\gamma(p_z^{C_1} + p_z^{C_2}) - \delta(p_z^{N_1} + p_z^{N_2})]$	$C_{1,2}$ -Ni- $N_{1,2}$ (π)
11	$d_{xy} + [\alpha(p_y^{C_1} + p_x^{C_2}) - \beta(p_y^{N_1} + p_x^{N_2})]$	$C_{1,2}$ -Ni- $N_{1,2}$ (π)
6	$d_{x^2-y^2} + \xi[(s^{C_1} - p_x^{C_1}) - (s^{C_2} - p_y^{C_2})]$	C_1 -Ni- C_2 (σ)
5	$+[(s^{C_1} - p_x^{C_1}) + (s^{C_2} - p_y^{C_2})]$	C_1 - C_2 (σ)
4	$d_{x^2-y^2} + \zeta[(s^{N_1} + p_x^{N_1}) - (s^{N_2} + p_y^{N_2})]$	N_1 -Ni- N_2 (σ)
3	$+[(s^{N_1} + p_x^{N_1}) + (s^{N_2} + p_y^{N_2})]$	N_1 - N_2 (σ)

to the three-center σ interactions. For short, finite tubes, the issue of interruption of interactions at the end of the tube will also be important. In this case, we expect the (n, \bar{n}) type to be the preferred structure for the following reasons: termination along $(n, 0)$ eliminates two σ interactions and two π interactions and distorts the remaining three-center σ interaction significantly; termination along (n, n) eliminates four σ interactions and four π interactions; and termination along (n, \bar{n}) eliminates only one σ interaction and two π interactions.

To support our qualitative analysis of the stability of cyanide nanotubes, which was based on the strength of bonds between atoms, we performed extensive total-energy calculations for the Pd(CN)₂ sheet and nanotubes; the results are shown in Table 2. From these results, we find that the infinite (4,4) and (4, $\bar{4}$) nanotubes have an energy 0.43 eV per Pd(CN)₂ unit lower than that of the (4,0) tubes, consistent with our analysis. Furthermore, we find that all three Pd(CN)₂ nanotubes are semiconductors with indirect gaps ranging from 2.1 to 2.8 eV. Compared to the sheet structure, the bandgap closes by 0.83 eV for the (4,0) tubes, and by 0.12 eV for both the (4,4) and (4, $\bar{4}$) tubes, which correspond to decreases of 28 and 4%, respectively, from the bandgap of the sheet. Note that the bandgap of these three nanotubes increases with the diameter, but is always smaller than the bandgap of the sheet. This feature is consistent with pre-

vious studies on MoS₂ nanotubes.^[13] This was further confirmed by additional calculations on (5,0) and (6,0) Pd(CN)₂ nanotubes. We find that the bandgaps of the fully relaxed (5,0) and (6,0) tubes are 2.66 and 2.56 eV, respectively. Both are larger than that of (4,0) tubes and smaller than that of the sheet. Interestingly, the (4,4) and (4, $\bar{4}$) tubes, which have a diameter larger than that of the (5,0) tube but smaller than that of the (6,0) tube, have larger bandgaps than

the square tubes. Considering that the $n=4$ nanotubes are those with the smallest possible diameter, we conclude that cyanide nanotubes have relatively stable bandgaps and uniform electronic properties. This is an essential element for practical applications. Compared to our cyanide nanotubes, the bandgaps of BNTs exhibit considerably larger relative variation with the tube diameter, while for CNTs the relative bandgap variation is even larger and the character of the system can easily change from semiconducting to metallic as a function of diameter and chirality changes.

2.3. Mechanical Features

We next consider the mechanical properties of the cyanide nanotubes. A quantitative description of the elasticity of the tubes requires calculation of Young's modulus, which involves specifying a wall thickness for the tubes. To our knowledge, there are different standards on how this quantity should be defined for nanotubes.^[13-15] Both the interlayer separation in the corresponding layered material (graphite for CNTs)^[13] and the average optimized intertube distance in periodic arrangements^[15] have been used as measures of the tube-wall thickness. Experimentally it has also been difficult to provide a precise value of Young's modulus for nanotubes.^[16-20] Previous theoretically and experimentally

Table 2. Structural and electronic properties of the Pd(CN)₂ sheet and nanotubes: ΔE is the energy difference of the tubes relative to the sheet per Pd(CN)₂ unit; ϵ_{gap} is the electronic bandgap; Pd-N, Pd-C, and C-N are the distances between pairs of atoms; D is the tube diameter; d is the intertube distance; Y is Young's modulus. The numbers in square brackets correspond to values in the periodic arrangement of tubes, and those without brackets to isolated tubes. The bond lengths of the (4,0) nanotube in the directions parallel and perpendicular to the axis are the same to within 0.01 Å.

	Sheet	(4,0) tube	(4, $\bar{4}$) tube	(4,4) tube
ΔE (eV)	0.00	0.56 [0.46]	0.13 [0.12]	0.13 [0.12]
ϵ_{gap} (eV)	2.96	2.13 [2.12]	2.83 [2.69]	2.82 [2.68]
Pd-N (Å)	2.03	2.05 [2.06]	2.04 [2.03]	2.04 [2.03]
Pd-C (Å)	1.94	1.94 [1.94]	1.94 [1.94]	1.94 [1.94]
C-N (Å)	1.17	1.17 [1.17]	1.17 [1.17]	1.17 [1.17]
D (Å)		7.08 [7.04]	8.95 [8.92]	9.07 [9.09]
d (Å)		[4.43]	[4.00]	[3.73]
Y (TPa)		0.23 [0.24]	0.06 [0.05]	0.03 [0.04]

determined values of Young's modulus fall within a range around 1 TPa for CNTs and around 0.8 TPa for BNTs.^[21] Recent experimental and theoretical work has provided a more comprehensive picture of the mechanical properties of various nanotubes.^[22–24] For the cyanide nanotubes, we use the intertube distance as the thickness of the tubes. To obtain this value, we considered a periodic arrangement of nanotubes on a hexagonal lattice in the plane perpendicular to their axis. In the optimal configuration, obtained from energy minimization, the intertube distance for the (4,0) nanotubes is 4.4 Å, for the (4,4) nanotubes is 4.0 Å, and for the (4, $\bar{4}$) nanotubes is 3.7 Å. The intertube interactions are weak (van der Waals type) and the energy in the periodic arrangement is lower than for isolated nanotubes by 0.1 eV for the (4,0) nanotubes, and by 0.01 eV for the (4,4) and the (4, $\bar{4}$) nanotubes per unit cell. Structural parameters for the three types of nanotube in the isolated and crystalline arrangement are summarized in Table 2. In general, the intertube interactions do not alter their structure or electronic properties.

The Young's modulus values listed in Table 2 for the cyanide–transition-metal nanotubes are more than one order of magnitude smaller than those of the CNTs and the BNTs reported in the literature. This finding is due to the fact that the cyanide nanotubes have much larger open spaces between rows of bonded atoms, which provide additional room for atomic relaxation when stress is applied, in contrast to the CNTs and BNTs where the very compact arrangement of atoms leaves little room for relaxation. The value of Young's modulus for the (4, $\bar{4}$) tubes is twice as large as that of the (4,4) tubes. This is due to the nature of the three-center σ bonds around the metal atom (M): the stretching of the (4, $\bar{4}$) tubes along the (n,n) direction, due to distortion brought about by the wrapping of the sheet into a tube, distorts both the C–M–C and N–M–N σ bonds, while the same operation on the (4,4) tubes along the (n,\bar{n}) direction helps to relax the distortions of those bonds, thus accounting for the large difference in the response of the two types of tube to external stress. This fact also supports our prediction that among the cyanide nanotubes with finite length, those of the (n,\bar{n}) type are likely to be the most stable.

3. Conclusions

Cyanide–transition-metal nanotubes could prove useful because of their structure-independent electronic structure as a function of size and chirality. By proposing and studying these tubes, we hope that this special property could be used for large-scale semiconducting-nanotube production and facilitate the use of these nanostructures as key elements in electronic-device applications. It is also straightforward to produce doped nanotubes, at least in principle. Specifically, by introducing acetylene (C₂H₂) in sufficient concentration instead of cyanide (HCN) at the second step of gas-phase synthesis, some CC units will be incorporated in the tube in place of the CN units to produce p-doped structures. By analogy, if N₂ molecules were introduced at the

second step of the gas-phase synthesis under the right conditions, some CN units would be replaced by NN units, thus giving rise to n-doped structures. However, due to the exceptional stability of the N₂ molecule, it may be significantly more difficult to produce n-doped tubes than p-doped tubes. Moreover, these tubes could also be easily functionalized because of the presence of several types of atom, in particular the metallic elements that can react more readily than the fully bonded C and N atoms. As our preceding analysis showed, both the valence-band maximum and the conduction-band minimum of the cyanide tubes have components from the d orbitals of the Pd atom. In particular, the highest-occupied band corresponds to a pure d_{3z²-r²} orbital, with lobes pointing out of the plane. This orbital would be available for interaction with orbitals of adsorbate atoms. Thus, doping of these semiconducting tubes may produce interesting variations of their electronic properties.

Acknowledgements

We thank I. Yavin, S. Lahili, and L. Jiang for technical help, L. Grant for a careful reading of the manuscript, Jie Xiang and his colleagues in the group of Prof. C. M. Lieber for suggestions on Ni(CN)₂ gas-phase synthesis, and M. Stopa for assistance with the electronic structure calculations. This work was supported in part by the Institute for Theory of Advanced Materials in Information Technology (ITAMIT) NSF Grant DMR-0325218, and in part by DOE CMSN Grant DE-FG02-05ER46226.

- [1] a) S. Iijima, *Nature* **1991**, *354*, 56–58; b) S. Iijima, T. Ichihashi, *Nature* **1993**, *363*, 603–605.
- [2] D. H. Cobden, M. Bockrath, P. L. McEuen, A. G. Rinzler, R. E. Smalley, *Phys. Rev. Lett.* **1998**, *81*, 681–684.
- [3] S. Frank, P. Poncharal, Z. L. Wang, W. A. de Heer, *Science* **1998**, *280*, 1744–1746.
- [4] A. Rubio, J. L. Corkill, M. L. Cohen, *Phys. Rev. B* **1994**, *49*, 5081–5084.
- [5] N. G. Chopra, R. J. Luyken, K. Cherrey, V. H. Crespi, M. L. Cohen, S. G. Louie, A. Zettl, *Science* **1995**, *269*, 966–967.
- [6] a) G. Kresse, J. Hafner, *Phys. Rev. B* **1993**, *47*, 558–561; b) G. Kresse, J. Furthmüller, *Phys. Rev. B* **1996**, *54*, 11 169–11 186.
- [7] N. A. W. Holzwarth, G. E. Matthews, A. R. Tackett, R. B. Dunning, *Phys. Rev. B* **1998**, *57*, 11 827–11 830.
- [8] a) J. P. Perdew, K. Burke, M. Ernzerhof, *Phys. Rev. Lett.* **1996**, *77*, 3865–3868; b) J. P. Perdew, K. Burke, M. Ernzerhof, *Phys. Rev. Lett.* **1997**, *78*, 1396–1399.
- [9] The default plane-wave cutoffs for the different elements are adopted. Gaussian smearing is applied to the electronic states near the Fermi level, with a width of 0.2 eV. Optimized atomic geometries are achieved when the forces on all unconstrained atoms are smaller in magnitude than 0.01 eVÅ⁻¹. A mesh in reciprocal space of 8×8×1 k points is used for sampling in the planar structure, and commensurate meshes for the tube structures.
- [10] L. Pauling, *The Nature of the Chemical Bond*, Cornell University Press, Ithaca, New York, **1960**, p. 170.
- [11] K. A. Hoffmann, F. Küspert, *Z. Anorg. Chem.* **1997**, *15*, 204.
- [12] a) J. H. Rayner, H. M. Powell, *J. Chem. Soc.* **1952**, 319; b) J. H. Rayner, H. M. Powell, *J. Chem. Soc.* **1958**, 3412.

- [13] G. Seifert, H. Terrones, M. Terrones, G. Jungnickel, T. Frauenheim, *Phys. Rev. Lett.* **2000**, *85*, 146–149.
- [14] J. P. Lu, *Phys. Rev. Lett.* **1997**, *79*, 1297–1300.
- [15] E. Hernández, C. Goze, P. Bernier, A. Rubio, *Phys. Rev. Lett.* **1998**, *80*, 4502–4505.
- [16] D. Sánchez-Portal, E. Artacho, J. M. Soler, A. Rubio, P. Ordejón, *Phys. Rev. B* **1999**, *59*, 12678–12688.
- [17] M. M. J. Treacy, T. W. Ebbesen, J. M. Gibson, *Nature* **1996**, *381*, 678–680.
- [18] A. Krishnan, E. Dujardin, T. W. Ebbesen, P. N. Yianilos, M. M. J. Treacy, *Phys. Rev. B* **1998**, *58*, 14013–14019.
- [19] J.-P. Salvetat, G. A. D. Briggs, J.-M. Bonard, R. R. Bacsa, A. J. Kulik, T. Stöcklin, N. A. Burnham, L. Forró, *Phys. Rev. Lett.* **1999**, *82*, 944–947.
- [20] N. G. Chopra, A. Zettl, *Solid State Commun.* **1998**, *105*, 297–300.
- [21] B. Akdim, R. Pachter, X. Duan, W. W. Adams, *Phys. Rev. B* **2003**, *67*, 245404.
- [22] M. Yu, B. S. Files, S. Arepalli, R. S. Ruoff, *Phys. Rev. Lett.* **2000**, *84*, 5552–5555.
- [23] M. Yu, O. Luorie, M. J. Dyer, K. Moloni, T. F. Kelly, R. S. Ruoff, *Science* **2000**, *287*, 637–640.
- [24] I. Kaplan-Ashiri, S. R. Cohen, K. Gartsman, V. Ivanovskaya, T. Heine, G. Seifert, I. Wiesel, H. D. Wagner, R. Tenne, *Proc. Natl. Acad. Sci. USA* **2006**, *103*, 523–528.

Received: January 16, 2007

Revised: March 2, 2007

Published online on May 15, 2007